Article

Residue-Based CaO Heterogeneous Catalysts from Crab and Mollusk Shells for FAME Production Via Transesterification

Claudia Cristina Cardoso, [ID] **,a Alexsandro S. Cavalcanti,a Ricardo O. Silva,b*
Severino Alves Junior,b Fabiana P. de Sousa,c Vânya Marcia D. Pasa,c
Santiago Ariasd and Jose G. A. Pachecod

aDepartamento de Química, Universidade Federal Rural de Pernambuco,
R. Dom Manoel de Medeiros, s/n, Dois Irmãos, 52171-900 Recife-PE, Brazil

bDepartamento de Química Fundamental, Universidade Federal de Pernambuco,
Av. Prof. José Rego, 1235, Cidade Universitária, 50740-540 Recife-PE, Brazil

cDepartamento de Química, Instituto de Ciências Exatas, Universidade Federal de Minas Gerais,
Avenida Antônio Carlos, 6627, Pampulha, 31270-901 Belo Horizonte-MG, Brazil

dLaboratório de Refino e Tecnologias Limpas (Lateclim-Litpeg),
Departamento de Engenharia Química, Universidade Federal de Pernambuco,
Av. Prof. José Rego, 1235, Cidade Universitária, 50740-540 Recife-PE, Brazil

The production of fatty acid methyl esther (FAME) via transesterification was studied, assessing the influence of CaO heterogeneous catalysts obtained from four different fishery residues: sururu, crab, clam and mussel. Characterization and properties of the residues were obtained via thermogravimetric analysis, X-ray diffraction, X-ray fluorescence, Fourier transform infrared (FTIR) spectra, nitrogen adsorption/desorption, chemical composition and scanning electron microscopy (SEM). Catalytic activities and reaction kinetics of FAME synthesis from the transesterification of soybean oil were performed. FAME yield was determined by ^{1}H nuclear magnetic resonance (NMR). A higher efficiency and reaction rate were observed for the catalysts obtained from the sururu residues with 93.7% FAME yield after 3.5 h of reaction at the first usage, reducing only to 91.0% after four consecutive cycles of reuse. The best activities were assigned to the presence of SrO, to smaller particle size, higher pore volumes and the higher Ca leaching, yielding Ca-diglyceroxide which is an important active phase for transesterification.

Keywords: FAME, fishery residues, heterogeneous catalyst, bivalve mollusks, CaO

Introduction

Among biofuels, biodiesel stands out for its potential for total or partial replacement of petroleum diesel. Biodiesel is a renewable, biodegradable, non-toxic, clean-burning fuel that produces low particulate emissions, has a high flash point, possesses better lubrication properties, has a high cetane number and is free of sulfur and aromatic compounds, and can be produced from waste and non-food sources.[1]

The most widely used method for obtaining biodiesel is transesterification. In this process, the triglycerides found in vegetable oils or animal fats react with methanol in the presence of a catalyst to produce a mixture of fatty acids methyl esters, named FAME, and glycerol. In order to meet the international standard of biodiesel, the FAME content has to be over 96.5%, apart from other parameters. In Brazil, biodiesel is produced from various oleaginous raw materials, but the most used are soybean oil, beef tallow and cottonseed oil. The soybean oil used for biodiesel corresponds to excess oil that does not compete with food production.[2-4]

The main industrial process of biodiesel production is alkaline transesterification with methanol in the presence of a homogenous sodium methylate catalyst. This process requires washing the biodiesel to remove the catalyst, producing soaps and decreasing the yield. The search for a heterogeneous catalyst may represent a decrease in the generation of effluents and an increase in yield.[5,6]

*e-mail: claudia_cardoso@ufrpe.br

Among the alkaline heterogeneous catalysts used in the synthesis of biodiesel, the alkaline earth metal oxides, hydrotalcites and basic zeolites stand out.[7] A large number of studies have been performed with calcium oxide (CaO) because of its economic advantages, high basicity, low solubility in alcohols, easy handling, excellent physicochemical activity, great catalytic activity and ease of acquisition.[8,9] CaO can be obtained from the heat treatment of nature-derived sources of $CaCO_3$ and from low-cost residues. The use of waste as calcium-based catalysts have been reported in the literature in the search for a more sustainable biodiesel production chain.[10–12]

Among the residual sources of calcium reported in the literature, are bones, eggshells, carapaces of snails and bivalve mollusks such as capiz, clams, oysters, mussels, and crustacean shells such as those of shrimp, prawns and crabs.[13-17] Among the sources cited, fishing residues are the most promising because of the demand and thus generation of high amount of waste.[18] The residues generated in fish processing plants correspond to approximately 50% of the fish weight, depending on the type of product and the processing techniques. A large part of these wastes is commonly disposed of in the open without any treatment over long periods of time, making this waste a serious environmental and public health problem.[19]

In Brazil, many coastal communities survive through artisanal fishing, and the residues of the shells are a national concern. However, there are no beneficiation projects for these materials. In 2011 alone, about 5,900 tons of bivalve mollusks were caught in this region.[20] Among the bivalve mollusks, the most important environmental concerns come from *Mytella falcata* (sururu), *Mytilus eduli* (mussel) and *Anomalocardia brasiliana* (clam), as well as the crustacean *Ucides cordatus* (crab).[21] Therefore, the residual carapaces of these species were chosen as objects of the present work.

This work studies the influence of four different types of Brazilian fishery residues with high calcium content (crab, sururu, mussel and clam shells) as sources of high active heterogeneous catalysts for FAME production from soybean oil via transesterification. The physicochemical and morphological characteristics of the catalysts were correlated with the activity. The use of these residues can contribute to environmentally friendly processes which decrease the volume of waste and help the production of biofuels.

Experimental

Materials

Commercial soybean oil (Liza®) was used without further purification. All the reagents and solvents were of analytical grade: methanol (99.8%, Vetec, Brazil), CaO (90.0%, Vetec, Brazil) and $CDCl_3$ containing 1% tetramethylsilane (TMS, D, 99.8%, CIL, USA). The shells of crustaceans and bivalve mollusks were obtained from the residual fishing process on the northeastern coast of Brazil. The residuals were cleansed with tap water and distilled water and dried in an oven at 100 °C for 1 h. After drying, the shells were ground in a ball mill and sifted through a 70-mesh sieve. The resulting thin powder was coded according to its source: $CaCO_3$-crab (*Ucides cordatus* crab), $CaCO_3$-clam (*Anomalocardia brasiliana* clam), $CaCO_3$-mussel (*Mytilus edulis* mussel) and $CaCO_3$-sururu (*Mytella falcate* mussel). The materials were calcined in a muffle furnace oven at 900 °C for 3 h, resulting in a thin white powder coded as CaO-crab, CaO-clam, CaO-mussel and CaO-sururu, respectively. These catalysts were maintained in a desiccator under vacuum until the time for the reaction.

Catalyst characterization

Thermogravimetric (TG) curves were obtained using a Shimadzu model DTG-60H thermobalance at a heating rate of 3 °C min^{-1}, from 10 to 900 °C, under nitrogen atmosphere with a gas flow of 100 mL min^{-1}. The X-ray diffractograms (XRD) were obtained using a Bruker diffractometer model D8 Advanced, Cu tube (Cu Kα, λ = 1.5418 Å), 30 kV voltage, 30 mA current, step of 0.02° and screening velocity of 5° min^{-1}, at a 2θ interval from 10 to 50°. The Fourier transform infrared attenuated total reflectance (FTIR-ATR) analyses were performed using a PerkinElmer, model Spectrum 400-FT-IR/FT-NIR spectrometer. The spectra were collected from 128 scans, resolution of 4 cm^{-1}, and wavelength range 4,000-400 cm^{-1}. Nitrogen isotherms were obtained using an autosorb Micromeritics apparatus, model 2420. Before the adsorption, the CaO catalysts were degassed at 120 °C for 8 h until they reached a pressure of 300 μm Hg. The specific surface areas were calculated according to the BET (Brauner, Emmett, Teller) method, varying P/P_0 = 0.05-0.30. The total volume of the pores was determined by measuring the quantity adsorbed at a relative pressure of 0.99. Scanning electron microscope (SEM) analyses were performed in a TESCAN MIRA 3 scanning microscope, with an accelerated 5 keV voltage. The samples had been previously treated by gold sputtering using the Sanyu Electron, model QUICK COATER SC-701, with a 6 mA current for 5 min during the metallization process. The elemental chemical composition of the samples was obtained by energy dispersive X-ray fluorescence spectroscopy using

a Rigaku NEX DE VS spectrometer 60 kV. For these analyses, two channels were used: Sr at a voltage of 35 kV and current of 300 mA, and NaCl at a voltage of 6.5 kV and current of 100 mA. The irradiation time for all the measurements was 100 s under helium atmosphere.

FAME synthesis and kinetic analysis

The transesterification reactions were performed using a 18:1 methanol:soybean oil molar ratio at reflux temperature under atmospheric pressure and with magnetic stirring of 400 rpm. The molar mass of soybean oil, based on its composition, was 1,288 g mol⁻¹, according to a previous publication.[22] The proportion of CaO catalyst used was 5% (mass/mass) relative to the mass of the soybean oil. The catalyst was stirred with methanol under reflux temperature for 1 h. The soybean oil, previously heated at 65 °C, was added to the mixture, and the reflux was continued. During the reactions, 1 mL aliquots were collected every 30 min. These aliquots were centrifuged at 500 rpm for 30 min to isolate the catalyst and glycerin. The residual alcohol present in the upper organic layer was removed by heating it in an oven at 100 °C for 1 h.

The resulting organic dry layer was analyzed by ¹H nuclear magnetic resonance (NMR) in a 300 MHz Varian Unity Plus 300 spectrometer with the samples dissolved in CDCl₃ and tetramethylsilane (TMS) as the internal reference standard. ¹H NMR analyses were performed for the quantification of FAME yield by monitoring the signals of the methoxyl and the α-CH₂ groups.[2]

First order kinetic model for triglyceride and methanol concentration was obtained based on equation 1.[23]

$$-\frac{d[TG]}{dt} = k[TG]^a \times [Me]^b \qquad (1)$$

where, $-\dfrac{d[TG]}{dt}$, k, [TG], [Me] are, respectively, triglyceride consumption rate, reaction rate constant, triglyceride and methanol concentrations. The exponents a and b are determined experimentally and they are related to the order of reaction for the triglyceride and methanol, respectively. In this work an excess of methanol:oil molar ratio of 18:1 was used to favor the transesterification reaction. An Eley-Riedel mechanism was considered, in which only methanol is adsorbed on the catalyst surface. The reversal reactions are not significant. Then the reaction rate is expressed in equation 2.

$$-\frac{d[TG]}{dt} = k\theta_{Me}[TG] \qquad (2)$$

where θ_{Me} is the coverage degree of the catalyst surface by methanol adsorption. As an excess of methanol was used, $k\theta_{Me}$ can be considered constant, and $k\theta_{Me} = k'$, in this aspect, the reaction rate can be simplified for a pseudo first order model as expressed in equation 3:

$$-\frac{d[TG]}{dt} = k'[TG] \qquad (3)$$

The equation 3 suggests that the transesterification reaction with methanol excess can be considered as a pseudo first order, as shown in the integrated equation (equation 4):

$$\ln\frac{[TG]}{[TG]_0} = k' \times t_f \qquad (4)$$

Considering that the amount of mono and diglycerides are not significant, equation 4 can be expressed as triglyceride conversion X (equation 5):

$$\ln(1-X) = k' \times t_f \qquad (5)$$

The apparent rate constants, k', were calculated by the slope of the lines obtained in the –ln(1 − X) *versus* time curves. The initial conversion was calculated between 0 and 1.5 h of transesterification reaction.

Reusability of the catalyst

To study the reusability of the catalyst, 100 g of soybean oil was heated with methanol at a molar ratio of 18:1 (methanol:soybean oil) and 5% (mass/mass) of the CaO-sururu catalyst under reflux for 3.5 h. The catalyst was removed through vacuum filtration, and the glycerin was separated through decantation. The filtered catalyst was then immediately weighed right away and transferred to another reaction flask containing methanol, without any pre-treatment, for reuse four times under the same reaction conditions. For each reaction, the excess methanol was removed from the resulting organic layer on a rotary evaporator at reduced pressure and analyzed by ¹H NMR to determine the FAME content.

The calcium content leached from the catalyst to FAME was determined using a methodology adapted from the literature,[24] in which 1 mL of sample was added to 25 mL of ethanol containing 1 mL of ammonium buffer solution (ca. pH 10) composed of NH₄Cl/NH₄OH. After homogenization, a small amount of Eriochrome T indicator was added under stirring until dissolution. The mixture was titrated with a standard 0.01 mol L⁻¹

ethylenediaminetetraacetic acid (EDTA) solution until the color turned from violet to blue. The calcium content was calculated by equation 6, in which Ca^{2+} is the calcium content; V is the volume of EDTA used in the titration; M is the EDTA molar concentration; MM is the molar mass of calcium and m is the mass of the sample.

$$\left[Ca^{2+}\right] = \frac{V \times M \times MM}{m} \qquad (6)$$

Results and Discussion

Characterization of fishery residues and catalysts

Thermogravimetric analysis of the fishery residues is shown in Figure 1. Three main stages of mass loss during the thermal decomposition process of the residues are observed, which is very common in this type of bivalve mollusk and crustacean shell.[15] These three stages are even more evident during the thermal decomposition of the crab ($CaCO_3$-crab).

The first stage of mass loss, present in all the samples up to 250 °C, refers to the elimination of water molecules and volatile organic materials present in the shells as a result of physisorption and chemisorption of molecules on the shells.[25] As can be seen in Table 1, these species were present in low quantities in the samples, except for the $CaCO_3$-crab, where there was a more significant mass loss below 400 °C, as was also observed in the work of Madhu *et al.*[26]

The second mass loss stage, between 250-600 °C, refers to the removal of water from $Ca(OH)_2$ and the decomposition of organic compounds.[15,26] This stage was observed in all the samples, being more pronounced in the carapaces of the crab. Because the crab is a crustacean, its shell contains a significant amount of the chitin and chitosan biopolymers.[25]

The third mass losses were observed in all the samples between 600 and 850 °C. At this stage, approximately 42% mass loss occurred in the bivalve mollusks (Table 1). Decomposition in this temperature range can be attributed to the transformation of $CaCO_3$ into CaO with the release of
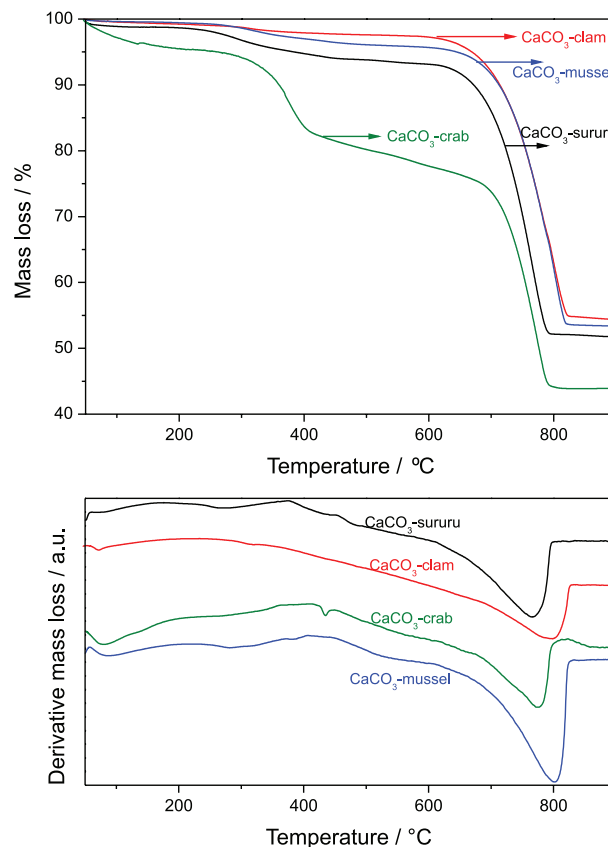

Figure 1. TG and derivative thermogravimetry (DTG) curves of fishery residues.

CO_2, which represents a stoichiometric loss of around 44% and corroborates the data from the literature.[15,25,26] In the case of $CaCO_3$-crab, the mass loss was about 34%, which is lower than the stoichiometric value due to the presence of other organic compounds, such as biopolymers.[25] For all samples, the mass loss stabilized at 830 °C. Then the calcination temperature was set to 900 °C to obtain the catalysts. After calcination, the CaO yields were about 43-57% for all materials (Table 1), which is similar to those reported in the literature.[27]

The diffractograms of the shells before calcination are shown in Figure 2. The diffractogram patterns for $CaCO_3$-clam were similar to the crystalline structure of the aragonite standard (power diffraction files (PDF) number 01-072-1650), a polymorph commonly found in

Table 1. Mass loss percentage from TG analysis and CaO yields after calcination of crab, sururu, mussel and clam shells

Sample	1st mass loss (50-250 °C) / %	2nd mass loss (250-600 °C) / %	3rd mass loss (600-825 °C) / %	Mass yield[a] / %
$CaCO_3$-sururu	2.0	5.0	41.5	51.8
$CaCO_3$-crab	4.9	17.4	33.8	49.7
$CaCO_3$-mussel	0.8	3.5	42.2	50.3
$CaCO_3$-clam	1.0	1.8	42.6	51.4

[a]Mass yield is the ratio between the sample amount and the CaO amount obtained after calcination.
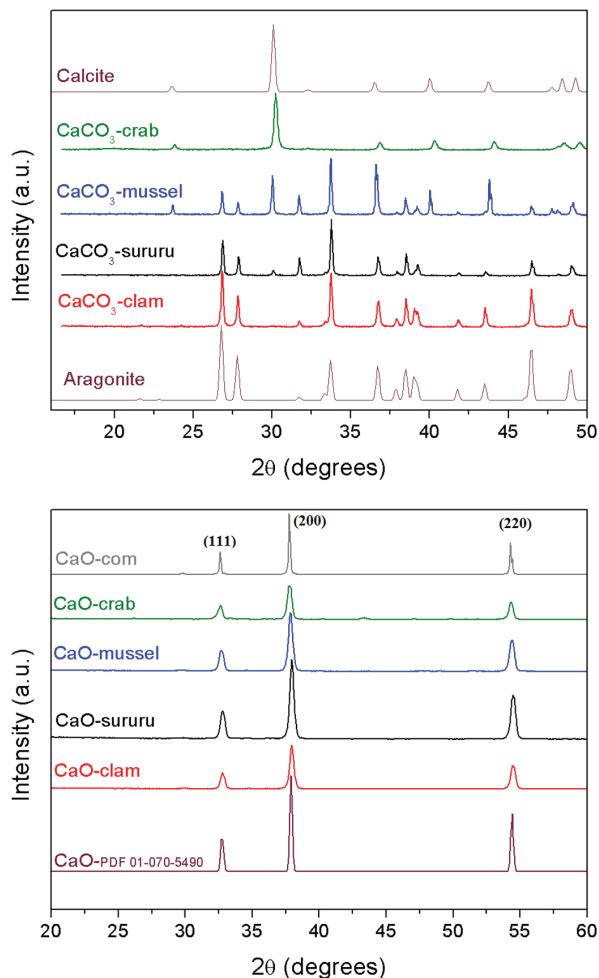
Figure 2. Diffractograms of fishery residues before calcination and CaO catalysts.

biologically produced $CaCO_3$ minerals.[27] This structure is different from that of the crustacean, $CaCO_3$-crab, which was similar to the calcite standard crystalline form (PDF number 01-072-1650). This result is compatible with other studies available in the literature.[28] $CaCO_3$-mussel and $CaCO_3$-sururu, however, presented reflections associated with a mixture of the crystalline patterns of aragonite and

calcite, as reported previously in mussel residues.[29] In both cases, the percentage of each phase was determined with the software Mach-3[30] showing 68% calcite and 32% aragonite for $CaCO_3$-mussel and 94% calcite and 6% aragonite for $CaCO_3$-sururu.

The diffractograms of the calcined samples (Figure 2) presented reflections in 2θ ca. 32.05°, 37.25° and 53.80°, characteristic of CaO (PDF number 01-070-5490) which demonstrates the success of calcinations and the carbonate conversion into oxide. Thus, regardless of the crystalline form of the original shell, all the oxides obtained possessed the same crystallographic form. The diffractogram of the CaO (CaO-com) obtained from a commercial $CaCO_3$, using the same calcination conditions (Figure 2) shows the same pattern as the diffractograms of the other CaO catalysts derived from the fishery residues. No additional phases containing calcium were detected in the oxides. Crystallite sizes of CaO were determined by the Scherrer equation. The results in Table 2 show that the calculated CaO crystallite size varied from 23.4 to 25.5 nm for all oxides except for the commercial CaO-com which was 59.9 nm. This fact suggest that the fishery residues are an effective way to obtain nanosized CaO crystallites. CaO crystallites in CaO-sururu and CaO-crab were slightly smaller than in CaO-mussel and CaO-clam (Table 2).

The FTIR-ATR spectra of the uncalcined shells are shown in Figure 3. The vibrational modes are attributed to asymmetric stretching $v_{as}(CO)$ at 1405 cm^{-1} for $CaCO_3$-crab, at 1450 cm^{-1} for $CaCO_3$-clam and $CaCO_3$-sururu, and at 1415 cm^{-1} for $CaCO_3$-mussel. Angular deformations outside the $\gamma(CO_3)$ plane are assigned to the 870 cm^{-1} band for $CaCO_3$-crab and at 860 cm^{-1} for the other samples.[14,31]

There is a displacement to lower frequency of the $v_{as}(CO)$ band and a displacement to a longer frequency of the $\gamma(CO_3)$ band in the $CaCO_3$-crab sample when compared to the spectra of the bivalve sururu, clam and mussel shells. This phenomenon can be attributed to the crystalline form of calcite because the $CaCO_3$-sururu and $CaCO_3$-clam

Table 2. Textural properties and composition of the CaO catalysts obtained after calcination of the fishery residues at 900 °C, compared with the CaO from the commercial $CaCO_3$

Catalyst	Surface area / (m² g⁻¹)	Pore volume / (cm³ g⁻¹)	Pore size / nm	Crystallite sizeᵃ / nm	CaOᵇ / %	MgOᵇ / %	SrOᵇ / %	Fe₂O₃ᵇ / %	Al₂O₃ᵇ / %	P₂O₅ᵇ / %	SiO₂ / %	S / %
CaO-sururu	3.2	0.0143	17.7	24.7	98.6	ND	0.39	0.02	0.60	ND	0.24	0.15
CaO-crab	3.5	0.0141	16.0	23.4	88.4	4.69	0.84	0.05	0.68	4.59	0.45	0.26
CaO-mussel	3.0	0.0131	17.6	25.5	98.9	ND	0.25	0.05	0.64	ND	ND	0.19
CaO-clam	2.8	0.0118	16.9	25.5	98.4	ND	0.29	0.23	0.67	ND	0.31	0.12
CaO-com	0.9	—	10.9	59.9								

ᵃCaO crystallite size from Scherrer equation in 220 oxides peak; ᵇcomposition from energy-dispersive X-ray spectroscopy (EDX) analyses; ND: not detectable.
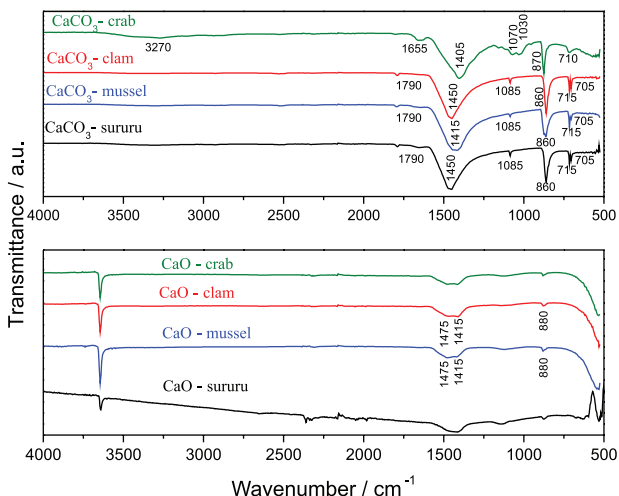
Figure 3. FTIR-ATR spectra of uncalcined fishery residues and CaO catalysts.

samples have an aragonite crystalline structure, as previously discussed in the XRD analysis. In addition, according to the XRD data, the $CaCO_3$-mussel consists of a combination of calcite and aragonite (Figure 2), which causes its $v_{as}(CO)$ frequency to lie between the values found for the $CaCO_3$-crab and the $CaCO_3$-sururu/$CaCO_3$-clam. The single band for the deformation in the plane $\delta(OCO)$ vibration at 710 cm^{-1} for the $CaCO_3$-crab sample (Figure 3) also confirms its crystalline structure as calcite, whereas the double peak at 705 and 715 cm^{-1} correspond to the aragonite structure for bivalve mollusks.

The 1085 cm^{-1} band (Figure 3) found in the three samples of the bivalve mollusks can be attributed to the symmetrical $v_s(C–O)$ vibration stretch of aragonite, a fact that agrees with the diffraction patterns. Meanwhile, the characteristic peak for this vibration is inactive in FTIR in the $CaCO_3$-crab sample, composed basically of calcite.[31] However, a double peak observed at 1030 and 1070 cm^{-1} is assigned to the stretching of the C–O–C group of the chitin biopolymer, commonly found in crustaceans and discussed in the TG analysis. The presence of chitin in the $CaCO_3$-crab can also be observed through the presence of the band at 1655 cm^{-1}, characteristic of the C=O of acetyl group in the secondary amide, and the band at 3270 cm^{-1}, resulting from the symmetrical stretching vibration of O–H groups overlapping the peak characteristic of the symmetrical N–H stretching vibrations.[25]

The FTIR-ATR spectra of the catalysts obtained from the calcination of residues of crab shells and bivalves are presented in Figure 3. In all spectra an absorption band near 530 cm^{-1}, characteristic of CaO was observed.[26] Also common to all the spectra is the band at 3645 cm^{-1}, which is attributed to the stretching vibration of hydroxyl groups that are bound to calcium as a result of the formation of

$Ca(OH)_2$, after exposure of the catalyst to moisture from air.[32] Infrared bands at 1415-1475 and 880 cm^{-1} may be assigned to $v2$ asymmetric stretching and $v3$ out-of-plane bend vibration of carbonate, respectively.[33] These bands indicate that some minimum amount of CO_2 was adsorbed on the catalyst surface after exposure to air.

The textural properties of the catalysts obtained from the calcination of the shells are shown in Table 2. The specific surface areas for all catalysts were approximately 3 m^2 g^{-1}, which is considered to be low but suitable for oxides. The pore sizes were about 17 nm for all catalysts which are compatible with the size of triglyceride to access the active sites of the catalyst. All samples presented low pore volumes. However, CaO-sururu and CaO-crab catalysts presented higher pore volume than CaO-clam and CaO-mussel. Also, the surface area of CaO-crab and CaO-sururu were slightly higher than CaO-mussel and CaO-clam catalysts. These results are in accordance with CaO crystallite size determined from XRD data. In this case, the smaller the crystallite size the higher the specific surface area. An important fact is that all catalysts presented a surface area higher than the commercial CaO which was 0.9 m^2 g^{-1}. Figure 4 shows that nitrogen adsorption-desorption isotherms for all CaO were type II, typical material with few pores, possibly because the catalysts had been subjected to high calcination temperatures.[34]

The chemical compositions of the shells of mollusks and crustaceans shell depend on the habitat of these species
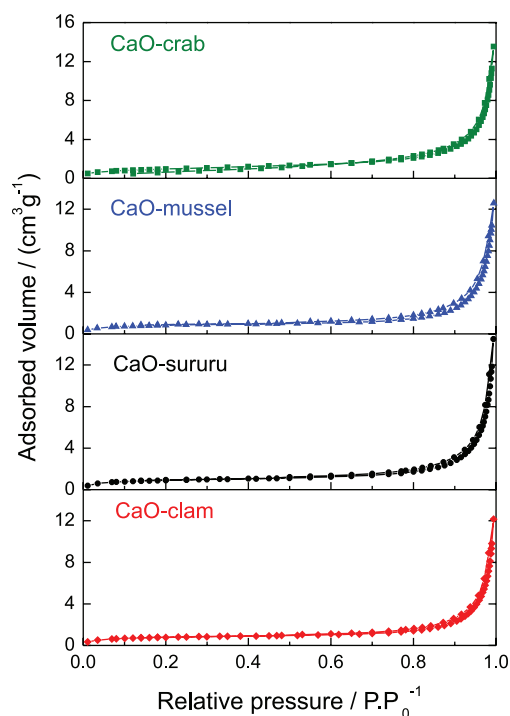

Figure 4. Isotherms of nitrogen adsorption and desorption of the CaO catalysts.

because many of these shells serve as environmental filterers that adsorb different metals. Table 2 shows that, as expected, all the catalysts were composed mostly of CaO. However, the presence of about 1% of some other metals was identified in the shells of all the bivalve mollusks (Table 2). The presence of sulfur identified in the CaO-mussel and potassium in the CaO-crab and CaO-clam samples has also been reported in the literature for other calcined shells.[14] A slighter higher strontium content was observed in the CaO-crab and CaO-sururu catalysts when compared to other samples. CaO-crab also presented a considerable amount of MgO (4.7%) and P_2O_5 (4.6%), which were not observed in any other catalyst in the present work. The presence of these considerable amount of MgO and P_2O_5 served to diminish the percentage amount of CaO.

A comparison of the SEM micrographs for crude shells ($CaCO_3$) and calcined catalysts (CaO) is presented in Figure 5. The rough shell morphologies (Figures 5a, 5c, 5e and 5g) possessed a compact and layered architecture of particles of irregular size with few evident surface pores.[15,28]

The catalysts (Figures 5b, 5d, 5f and 5h) presented smaller particle sizes than the original shell samples (Figures 5a, 5c, 5e and 5g) which agree with results reported in the literature.[26] The irregular morphology of the calcined catalysts may be attributed to the high calcination temperature.[26] These changes are mainly a result of the volatilization of the organic materials present in the shell matrices during the calcination process, in addition to the release of the CO_2 from the surface as a result of the $CaCO_3$ decomposition to form CaO.[35] A cauliflower or honeycomb morphology can be seen in the surface of CaO-crab catalysts (Figure 6b) when compared to $CaCO_3$-crab (Figure 6a). This fact is probably due to the release of many molecules (biopolymers, H_2O, CO_2) during the calcination process.

Among the catalysts studied, the CaO-clam had a higher particle size than the others (Figure 5f). This fact may have influenced the catalytic activity of this catalyst, because the higher particle size of the catalyst, smaller the surface area, making it difficult for the molecule to access the active sites.[34] These results confirmed that differences in the CaO morphology depend on the origin of the $CaCO_3$, thus resulting in distinct transesterification yields.

Transesterification of soybean oil over CaO catalysts

In a previous work,[34] we studied the use of CaO as a heterogeneous catalyst using $CaCO_3$ from an eggshell residual source. Immediately before the reaction, $CaCO_3$ needs to be calcined to CaO and quickly used to avoid transformations that can reduce its activity.[10,36] In order to obtain greater flexibility in the handling of the catalyst, in the present work a larger amount of CaO was produced from fishery residues, and placed in a desiccator under vacuum to prevent a reaction with moist air forming $Ca(OH)_2$, and reaction with CO_2 from the atmosphere, producing $CaCO_3$. Prior to the reaction, the CaO was
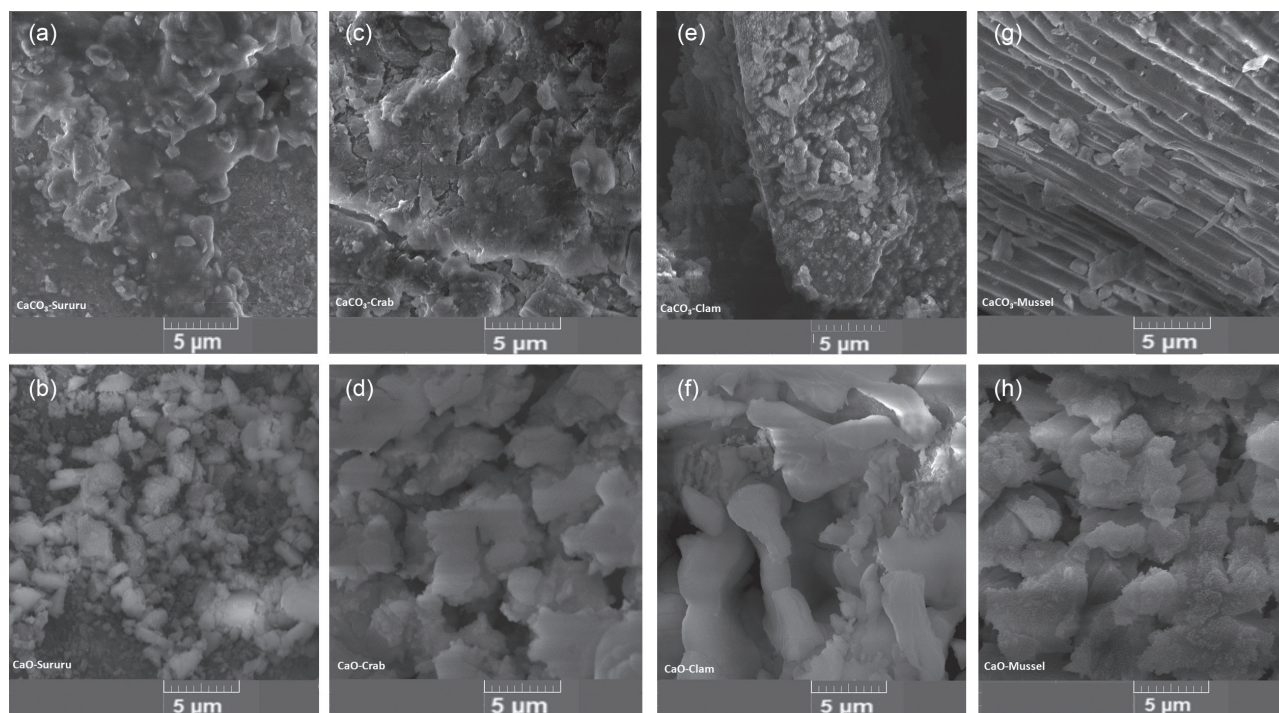

Figure 5. SEM micrographs of (a) sururu, (c) crab, (e) clam and (g) mussel fishery residues and CaO (b) sururu, (d) crab, (f) clam and (h) mussel catalysts obtained after calcination.
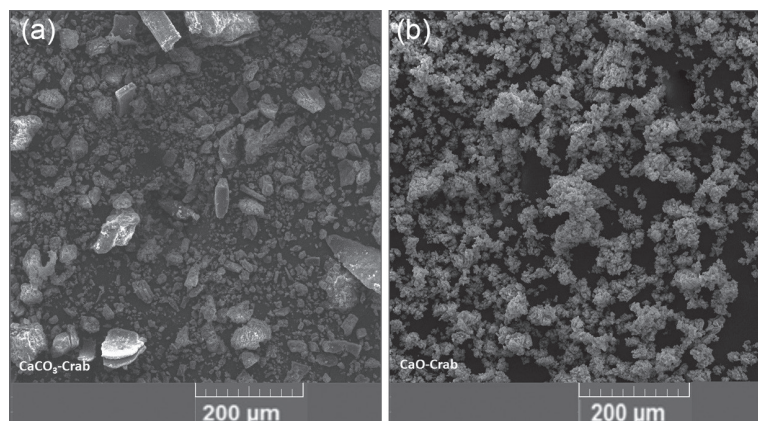
Figure 6. SEM comparison of (a) CaCO$_3$-crab shell and (b) CaO-crab catalyst.

preactivated in the presence of methanol under reflux for 1 h before the addition of the soybean oil. At this time, any potential amount of Ca(OH)$_2$ present on the CaO surface was dissolved and the catalyst was activated.[8,37,38] For this reason, based on literature, an excess of catalyst was used in a ratio of 5 mass% to soybean oil, considering any possible loss of CaO as Ca(OH)$_2$ during the storage and activation of the catalyst.[15,34,37]

The alcohol:oil molar ratio is one of the most important factors affecting the conversion to FAME. Although the stoichiometric ratio is 3:1, the transesterification reaction is reversible and therefore requires excess methanol to favor the formation of FAME.[39-41] Excess methanol increases the formation of calcium methoxide (Ca-Met) on the surface of the catalyst, which shifts the equilibrium to the products.[14] However, proportions of methanol:oil greater than 20:1 speed up the formation of biodiesel and glycerol. Thus, after formation of an appreciable amount of glycerol, there is a reaction with the CaO active sites, producing calcium glyceride (Ca-Gly) which is less active than CaO for transesterification.[27,40] Therefore, it is important to maintain a high methanol:oil molar ratio, but below 20:1.

The proposed international method for determining the FAME content in biodiesel is by using the gas chromatograph with flame ionization detector (GC-FID) technique which must meet the specifications of the standards EN 14214[42] and CNS 15072[43] standards. However, a kinetic study of transesterification needs to analyze samples of low conversion sample with low ester content in the presence of unconverted vegetable oil, which can damage the GC-FID analysis system. Therefore, we used the ^{1}H NMR spectroscopic technique to quantify the yield to FAME in several samples withdrawn throughout the reaction.[2] Figure 7 shows the ^{1}H NMR (300 MHz, CDCl$_3$) spectra of the soybean oil and one sample of partially converted triglycerides to FAME used to determine the FAME yield.

FAME yields for the methylic transesterification of soybean oil over CaO catalyst as a function of reaction time are shown in Figure 8. Results show that with the CaO-sururu, CaO-crab, CaO-clam and CaO-mussel catalysts, the FAME yields were 93.7, 86.3, 81.0 and 79.3%, respectively, after 3.5 h of reaction (Figure 8). The yield with the pure CaO-com was around 93%, the same as the best catalyst CaO-sururu, after 3.5 h of reaction. In the case of the reaction using CaO-sururu, however, the FAME yield was 89.0% after only one hour of reaction. This value was much higher than the yield from the other catalysts: 50.7% for CaO-crab, 21.7% for CaO-mussel, 10.7% for CaO-com and 3.3% for CaO-clam catalysts, after the same reaction time.

The initial reaction rate, obtained from the slope of the FAME yield curve from 0 to 1.5 h, for the CaO-sururu catalyst was the most accentuated, followed by those for the CaO-crab, CaO-mussel, CaO-com and CaO-clam catalysts (Figure 8). This fact suggests that the initial rate of the transesterification reaction of soybean oil using the catalysts from the different sources follows the following order: CaO-sururu > CaO-crab > CaO-mussel > CaO-com > CaO-clam. The values of the apparent reaction rate constants, k', calculated from the plot of the linearized reaction rate equation $-\ln(1-X)$ *versus* time (min) curves in the range 0 to 90 min (Supplementary Information section), presented these values: 0.0207 min^{-1} for CaO-sururu, 0.0105 min^{-1} for CaO-crab , 0.0041 min^{-1} for CaO-mussel, 0.0026 min^{-1} for CaO-com and 0.0004 min^{-1} for CaO-clam. The result of low reaction rate obtained for the CaO-com can be explained by its higher CaO crystallite size which resulted in the smaller surface area (Table 2).

The apparent reaction rate constant obtained in the present work for CaO-sururu (0.0207 min^{-1}) and for CaO-crab (0.0105 min^{-1}) catalysts was much higher than those described in other works that have studied the transesterification of soybean oil using CaO as catalyst
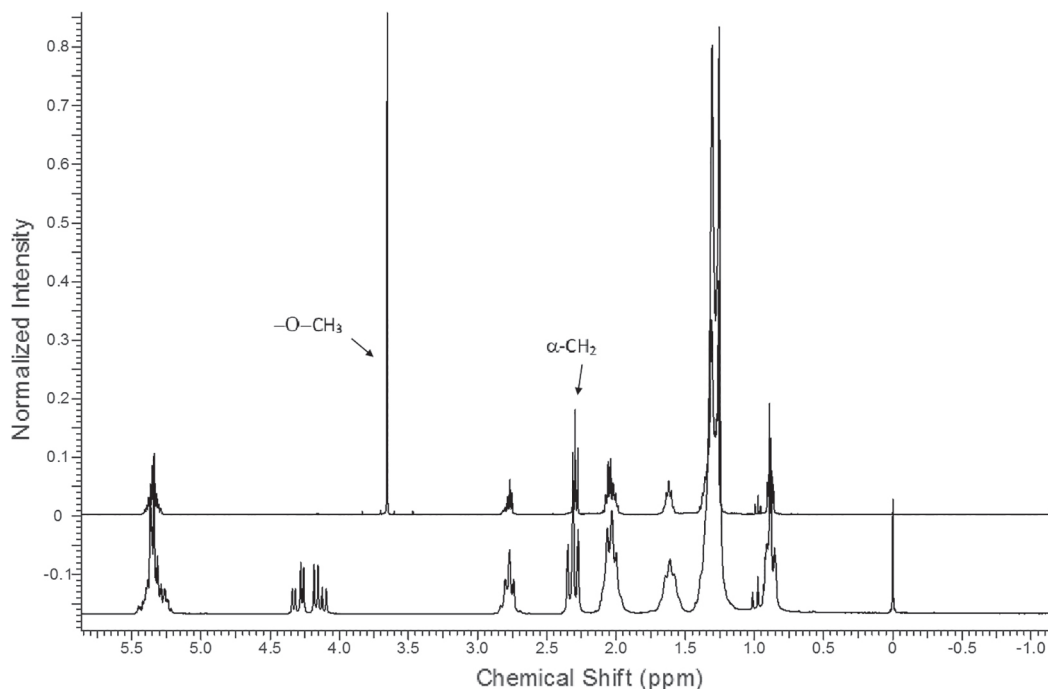
Figure 7. ^{1}H NMR (300 MHz, CDCl₃) spectrum of soybean oil and its respective FAME.
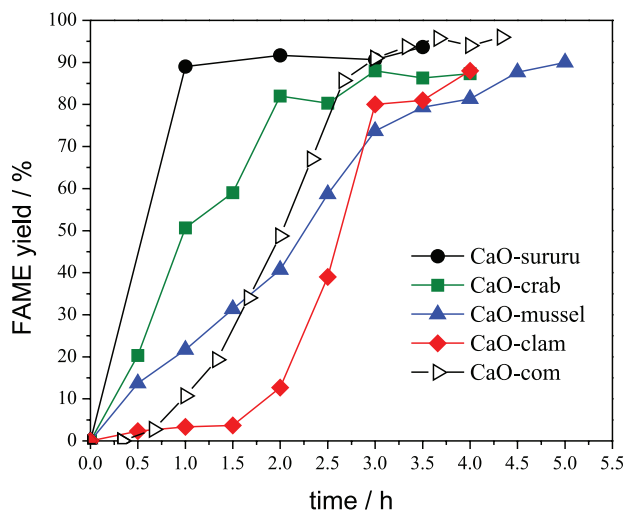

Figure 8. Fatty acid methyl ester (FAME) yields for the transesterification of soybean oil over catalysts. Methanol:oil molar ratio = 18:1, temperature = 65 °C at reflux, catalyst concentration = 5 mass%.

from different residue sources. For instance, CaO from chicken eggshells gave a rate constant of 0.006 min⁻¹.[34] KI impregnated on CaO from calcined oyster shells gave 0.0073 min⁻¹.[35] The FAME yield obtained in the present work was also much higher than the yield obtained with CaO from oyster shells (74%) for soybean transesterification under optimized conditions.[13]

Significant catalytic activities in the transesterification of soybean oil were observed for all of the catalysts in spite of their apparent reaction rate k' constants. We can relate the best catalytic activity for CaO-sururu and CaO-crab

catalysts to the fact that these catalysts have higher surface areas and pore volumes (Table 2), smaller CaO crystallite sizes (Table 2) and smaller particle sizes (Figures 5b and 5d), which make their active sites more readily available. Also, these morphological characteristics permitted more leaching of Ca, yielding more Ca-diglyceroxide, which is consider an important active species for the transesterification reaction, as previously reported.[10,34] The least efficient catalyst was CaO-clam, which has a larger particle size (Figure 5F). Another factor that might have contributed to the greater activity of the CaO-sururu and CaO-crab catalysts is the presence of Sr in slightly higher amounts than in the other two catalysts, as observed in the X-ray fluorescence analysis (Table 2). According to Kouzu *et al.*,[10,44] SrO has higher basic strength than CaO. In our case, the content of SrO in the catalysts ranged from 0.30 to 0.84 mass%, while the CaO content ranged from 88.4 to 98.9 mass%. Although the basicity of the catalysts is not significantly affected due to the high CaO percentage, the presence of small amount of SrO may have contributed to the higher catalytic activity of CaO-sururu and CaO-crab catalysts. Apart from the fact that the amount of SrO is slightly higher for the CaO-crab compared to CaO-sururu, an amount of 4.7% MgO in CaO-crab was observed. Also, the content of CaO was 84.8 mass% in CaO-crab and 98.6% in CaO-sururu. According to Kouzu *et al.*[44] for the transesterification using alkaline-earth metal oxides, the catalytic activity for FAME followed the order MgO << CaO < SrO, which can explain why the CaO-crab

had a worse catalytic activity than CaO-sururu even with a smaller amount of SrO.

As the specific area and porosity of the catalysts tested presented similar values (Table 2), it is believed that these parameters did not significantly interfere in the final FAME yield after 3 h of reaction. As none of the catalysts studied exhibited significant porosity, the phenomena of internal diffusion should not be very significant. The kinetics of the CaO-sururu and CaO-crab catalysts, nonetheless, were much faster than the other catalysts. Catalysts with high kinetic rates are preferable as they require a smaller industrial reactor to produce biodiesel. As all the catalysts studied did not exhibit significant porosity, the phenomena of internal diffusion should not be very significant. On the other hand, this fact implies in a reduced specific surface area thus requiring a higher concentration of catalyst in relation to the oil mass. As the catalysts in the present work were obtained from a residual fishery industry with high availability at low cost, these materials are suitable for large scale biodiesel production even in high concentrations.

Reuse of the catalyst

One of the advantages presented by the heterogeneous catalysts, compared to the homogeneous catalysts, is that they can be reused several times. Furthermore, after loss of their catalytic activities, these catalysts can be regenerated or used for various other purposes, such as building materials, soil stabilizers, cement industries and phosphate adsorbents.[45]

The transesterification kinetics of soybean oil was best obtained from the CaO-sururu catalyst. FAME yields as a function of reaction time are shown in Figure 9 for four cycles of reaction. The FAME content decreased from 89.0 to 79.3% from the first to the second cycle, followed by 66.7 and 45.0% in the third and fourth cycles, respectively, after 1 h of reaction (Figure 9). Thus, the rates of the transesterification reactions decreased with the increase in the number of cycles to which the catalyst was subjected. The apparent rate constants, k", were calculated in the period of 0 to 2 h and confirmed the decrease in reaction velocity with increasing number of catalyst cycles, presenting these values: 0.0207 min^{-1} for the 1st cycle, 0.0177 min^{-1} for the 2nd cycle, 0.0143 min^{-1} for the 3rd cycle, 0.0101 min^{-1} for the 4th cycle. Despite the decrease in the reaction rate with the increase in the number of cycles, the FAME yields reached approximately 91% in all four cycles after 3 h of reaction. After 3.5 h of reaction the FAME yield of the 4th cycle was 84% that is slightly lower than the yield of 92% in the first cycle. This result is even higher than those reported in some published studies.

As an example, Lee *et al.*,[46] Sirisomboonchai *et al.*[47] and Syazwani *et al.*[27] obtained yields of about 30, 66 and 80%, respectively, after four cycles of reuse of the CaO catalyst obtained from *C. obtusa*, scallop shells and *Tapes belcheri* S., respectively.
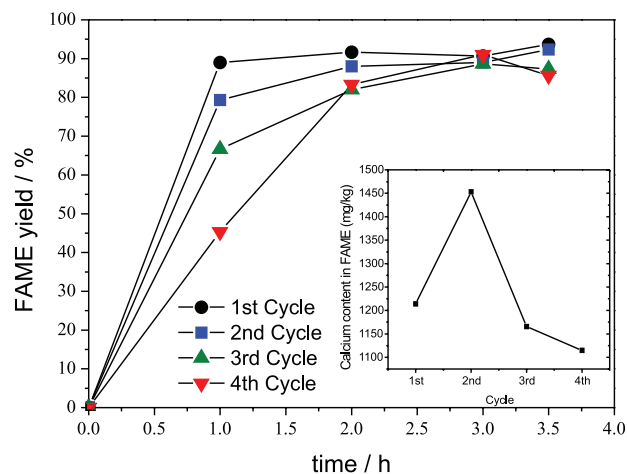

Figure 9. FAME yield kinetics for the transesterification of soybean oil over CaO-sururu catalyst during four cycles of reaction and calcium contents in FAME. Insert: the amount of Ca^{2+} leached from the CaO-sururu catalyst during the 4 cycles.

The loss of activity by the CaO-sururu catalyst along the cycles may be related to the formation of Ca(OH)$_2$ on the surface because of the presence of moisture in the vegetable oil. CaO has a higher basic strength than Ca(OH)$_2$ because the former has strong Lewis base sites, which justifies the lower catalytic activity of Ca(OH)$_2$.[5]

The amount of Ca^{2+} leached from the CaO-sururu catalyst was accomplished by complexometric titration to determine the Ca^{2+} content in FAME product at the end of each of the 4 cycles (insert in Figure 9). The presence of Ca^{2+} in the FAME indicates an important leaching of the catalyst. It has been reported that the transesterification of vegetable oil is catalyzed not only by the heterogeneous basic sites of the CaO surface, but also in a smaller amount by the leached compounds leaving the CaO catalyst, which corresponds to a homogeneous contribution favorable to the reaction.[44,48] Despite the leaching of the catalyst throughout the reaction, previous studies from our group have demonstrated an effective heterogeneous catalytic action on the part of the CaO.[34] At the end of the process, further removal of Ca^{2+} from the FAME produced could be done in the purification process step by water washing or by the use of ion exchange resins.[49] The results recorded in Figure 9 (insert) show that the amount of leached Ca^{2+} reduced as the number of reuse cycles increased, with consequent reduction of FAME content. These data corroborate the importance of small size particle and high

surface area of the catalyst for Ca^{2+} leaching, increasing the performance in this process.

From the results obtained in the present work, to obtain a product with specification of biodiesel using the best CaO-sururu catalyst, it would be necessary to carry out further studies involving the following steps: (*i*) to perform experiments at higher temperatures, varying the temperature in a pressurized reactor, since the boiling temperature of methanol is 65 °C; (*ii*) to optimize the percentage of catalyst; (*iii*) to optimize the methanol:oil ratio; (*iv*) to study the purification of the final product to remove the residues of total glycerol, methanol and leached calcium; (*v*) to perform mass balances to obtain biodiesel yield in relation to vegetable oil feed, and the amount of consumed mass of catalyst and methanol *per* kg of biodiesel produced.

Conclusions

An ecologically destination for tons of fishery waste generated along the Brazilian coast may be obtained by the use of these wastes to produce catalysts. The catalysts obtained from the calcination of sururu, crab, clam and mussel shell residues were composed of more than 97% of CaO. The catalysts derived from fishery residues catalyzed a methylic transesterification of soybean oil obtaining FAME yields between 79 and 94% after 3.5 h of reaction. In the case of the CaO-sururu reaction, 89.0% of FAME yield was observed after only 1 h of reaction, while the other catalysts led to a FAME yield less than 50% in the same reaction time. These results show that the origin of the residues have a significant influence on the performance of the catalyst. Catalysts obtained from crab and sururu shells had more SrO and smaller particle size which might be responsible for the higher activity of these catalysts. The higher specific surface areas and pore volumes of these catalysts were also attributed to the greater activity, as well as the formation of Ca-diglycerides as active species. The reuse of the CaO-sururu catalyst led to a yield FAME of 91% after 3 h of reaction, after four consecutive reuses with no previous treatment between one reaction and another. These results confirm the catalytic potential for the production of catalysts derived from fishery residues in the production of FAME via transesterification of soybean oil. To meet standards for biodiesel production, 96.5% FAME is required, which means that better reaction conditions still need to be investigated. Besides this, the use of these recycled waste materials may not only contribute to a more economical and sustainable production of biodiesel, but also promote environmental benefits to obtain a cleaner process with fewer stages of purification compared to the conventional process based on homogeneous alkaline catalysis. In addition, the use of fishery waste can generate extra income for fishers of crabs and mollusks, with social and economic benefits.

Supplementary Information

The plot of the linearized reaction rate equation $-\ln(1 - X)$ *versus* time (min) curves in the range 0 to 90 min is available free of charge at http://jbcs.sbq.org.br as PDF file. Those curves were used to determinate the rate constants, k', for the catalysts studied.

Acknowledgments

References

1. Hoekman, S. K.; Broch, A.; Robbins, C.; Ceniceros, E.; Natarajan, M.; *Renewable Sustainable Energy Rev.* **2012**, *16*, 143.

2. Cardoso, C. C.; Mendes, B. M. O.; Pasa, V. M. D.; *J. Environ. Chem. Eng.* **2018**, *6*, 2241.

3. Cremonez, P. A.; Feroldi, M.; Nadaleti, W. C.; de Rossi, E.; Feiden, A.; de Camargo, M. P.; Cremonez, F. E.; Klajn, F. F.; *Renewable Sustainable Energy Rev.* **2015**, *42*, 415.

4. Rico, J. A. P.; Sauer, I. L.; *Renewable Sustainable Energy Rev.* **2015**, *45*, 513.

5. Baskar, G.; Aiswarya, R.; *Renewable Sustainable Energy Rev.* **2016**, *57*, 496.

6. Shan, R.; Lu, L.; Shi, Y.; Yuan, H.; Shi, J.; *Energy Convers. Manage.* **2018**, *178*, 277.

7. Kawashima, A.; Matsubara, K.; Honda, K.; *Bioresour. Technol.* **2008**, *99*, 3439.

8. Kawashima, A.; Matsubara, K.; Honda, K.; *Bioresour. Technol.* **2009**, *100*, 696.

9. Bankovi, I. B.; Miladinovi, M. R.; Stamenkovi, O. S.; Veljkovi, V. B.; *Renewable Sustainable Energy Rev.* **2017**, *72*, 746.

10. Kouzu, M.; Hidaka, J.; *Fuel* **2012**, *93*, 1.

11. Catarino, M.; Ramos, M.; Dias, A. P. S.; Santos, M. T.; Puna, J. F.; Gomes, J. F.; *Waste Biomass Valorization* **2017**, *8*, 1699.

12. Liu, X.; He, H.; Wang, Y.; Zhu, S.; Piao, X.; *Fuel* **2008**, *87*, 216.

13. Nakatani, N.; Takamori, H.; Takeda, K.; Sakugawa, H.; *Bioresour. Technol.* **2009**, *100*, 1510.

14. Boro, J.; Thakur, A. J.; Deka, D.; *Fuel Process. Technol.* **2011**, *92*, 2061.

15. Hu, S.; Wang, Y.; Han, H.; *Biomass Bioenergy* **2011**, *35*, 3627.

16. Girish, N.; Niju, S. P.; Mohamed, K.; Sheriffa, M.; *Fuel* **2013**, *111*, 653.

17. Rezaei, R.; Mohadesi, M.; Moradi, G. R.; *Fuel* **2013**, *109*, 534.

18. Kerton, F. M.; Liu, Y.; Omari, K. W.; Hawboldt, K.; *Green Chem.* **2013**, *15*, 860.

19. Islam, S.; *Mar. Pollut. Bull.* **2004**, *49*, 103.

20. Silva, T. S.; Meili, L.; Carvalho, S. H. V.; Soletti, J. I.; Dotto, G. L.; Fonseca, E. J. S.; *Environ. Sci. Pollut. Res.* **2017**, *24*, 19927.

21. Vasconcellos, M.; Diegues, A. C.; Kalikoski, D. C. In *Coastal Fisheries of Latin America and the Caribbean*; Salas, S.; Chuenpagdee, R.; Charles, A.; Seijo, J. C., eds.; Food and Agriculture Organization of the United Nations (FAO): Rome, 2011, p. 73-116. Available at http://www.fao.org/3/a-i1926e.pdf accessed in October 2019.

22. Prado, R. G.; Almeida, G. D.; de Oliveira, A. R.; de Souza, P. M. T. G.; Cardoso, C. C.; Constantino, V. R.-L.; Pinto, F. G.; Tronto, J.; Pasa, V. M. D.; *Energy Fuels* **2016**, *30*, 6662.

23. Al-Sakkari, E. G.; El-Sheltawy, S. T.; Attia, N. K.; Mostafa, S. R.; *Appl. Catal., B* **2017**, *206*, 146.

24. Pereira, C. M.; Neiverth, C. A.; Maeda, S.; Guiotoku, M.; Franciscon, L.; *Rev. Bras. Ciênc. Solo* **2011**, *35*, 1331.

25. Correia, L. M.; Saboya, R. M. A.; Campelo, N. D.; Cecilia, J. A.; Rodriguez-Castellon, E.; Cavalcante, C. L.; Vieira, R. S.; *Bioresour. Technol.* **2014**, *151*, 207.

26. Madhu, D.; Chavan, S. B.; Singh, V.; Singh, B.; Sharma, Y. C.; *Bioresour. Technol.* **2016**, *214*, 210.

27. Syazwani, O. N.; Teo, S. H.; Islam, A.; Taufiq-Yap, Y. H.; *Process Saf. Environ. Prot.* **2017**, *105*, 303.

28. El-Gendy, N. S.; Hamdy, A.; Abu Amr, S. S.; *Int. J. Biomater.* **2014**, *2014*, ID 609624.

29. Tekin, K.; *Energy Fuels* **2015**, *29*, 4382.

30. *Mach-3*; Newfangled Solutions, Livermore Falls, USA, 2008.

31. Andersen, F. A.; Brečević, L.; *Acta Chem. Scand.* **1991**, *45*, 1018.

32. Chen, G.; Shan, R.; Shi, J.; Yan, B.; *Bioresour. Technol.* **2014**, *171*, 428.

33. Fleet, M. E.; *Biomaterials* **2009**, *30*, 1473.

34. de Sousa, F. P.; dos Reis, G. P.; Cardoso, C. C.; Mussel, W. N.; Pasa, V. M. D.; *J. Environ. Chem. Eng.* **2016**, *4*, 1970.

35. Jairam, S.; Kolar, P.; Sharma-shivappa, R.; Osborne, J. A.; Davis, J. P.; *Bioresour. Technol.* **2012**, *104*, 329.

36. Chen, G.; Shan, R.; Shi, J.; Yan, B.; *Fuel Process. Technol.* **2015**, *133*, 8.

37. Boro, J.; Konwar, L. J.; Deka, D.; *Fuel Process. Technol.* **2014**, *122*, 72.

38. Piker, A.; Tabah, B.; Perkas, N.; Gedanken, A.; *Fuel* **2016**, *182*, 34.

39. Roschat, W.; Siritanon, T.; Yoosuk, B.; Promarak, V.; *Energy Convers. Manage.* **2016**, *108*, 459.

40. Margaretha, Y. Y.; Prastyo, H. S.; Ayucitra, A.; Ismadji, S.; *Int. J. Energy Environ. Eng.* **2012**, *3*, 33.

41. Muciño, G. G.; Romero, R.; Ramírez, A.; Martínez, S. L.; Baeza-Jiménez, R.; Natividad, R.; *Fuel* **2014**, *138*, 143.

42. EN 14214: *Automotive Fuels – Fatty Acid Methyl Esters (FAME) for Diesel Engines-Requirements and Test Methods*; European Committee for Standardization (CEN): Brussels, 2003.

43. Bureau of Standards, Metrology and Inspection of Taiwan (TBOS); *CNS 15072*; Chinese National Standards (CNS): Taiwan, 2010.

44. Kouzu, M.; Kasuno, T.; Tajika, M.; Sugimoto, Y.; Yamanaka, S.; Hidaka, J.; *Fuel* **2008**, *87*, 2798.

45. Lam, M. K.; Lee, K. T.; Mohamed, A. R.; *Biotechnol. Adv.* **2010**, *28*, 500.

46. Lee, S. L.; Wong, Y. C.; Tan, Y. P.; Yew, S. Y.; *Energy Convers. Manage.* **2015**, *93*, 282.

47. Sirisomboonchai, S.; Abuduwayiti, M.; Guan, G.; Samart, C.; *Energy Convers. Manage.* **2015**, *95*, 242.

48. Granados, M. L.; Poves, M. D. Z.; Alonso, D. M.; Mariscal, R.; Galisteo, F. C.; Moreno-Tost, R.; Santamaria, J.; Fierro, J. L. G.; *Appl. Catal., B* **2007**, *73*, 317.

49. Alba-Rubio, A. C.; Alonso Castillo, M. L.; Albuquerque, M. C. G.; Mariscal, R.; Cavalcante, C. L.; Granados, M. L.; *Fuel* **2012**, *95*, 464.